Journal of Nuclear Materials 122 & 123 (1984) 66-79
North-Holland, Amsterdam

MATERIALS FOR IMPURITY CONTROL

Richard F. MATTAS, Dale L. SMITH, and Mohamed A. ABDOU

Argonne National Laboratory, Fusion Power Program, 9700 South Cass Avenue, Argonne, IL 60439

The materials data base for candidate impurity control materials is reviewed. The plasma side materials considered are Be, C, SiC, TiC, and W, and the heat sink materials considered are copper alloys and vanadium alloys. The properties which are evaluated are physical and chemical sputtering, bulk properties, and irradiation properties. Design implications on design are also discussed.

1. INTRODUCTION

Impurity control components, including limiter blades, divertor collector plates, and halo scraper plates, are exposed to high particle fluxes that can result in high sputtering erosion rates and high heat fluxes. In addition, the materials are exposed to high neutron fluxes which will degrade the bulk properties. The structures must be resistant to erosion losses and radiation damage, capable of operating at elevated temperatures, and environmentally compatible with the surroundings.

There is a large number of properties that are important for the materials selection, as shown in Table 1. The desired thermophysical properties are those that minimize the thermal stresses. The mechanical strength and ductility should be adequate to accommodate the weight loads, coolant pressures, thermal stresses, and electromagnetic forces. For high cycle machines, the materials should exhibit good fatigue, crack growth, and stress corrosion behavior. The materials should also exhibit low swelling and creep during irradiation. The surface sputtering rates should be low enough to provide extended lifetimes and to keep the impurities at acceptable levels in the plasma. A survey of available materials indicates that no one material is capable of satisfying both the surface sputtering and the structural requirements. Hence, the designs of impurity control components incorporate separate plasma side materials which are attached to a structural material selected to meet the strength and radiation damage requirements. The division of plasma side and structural materials allows greater flexibility in the selection of materials, but also creates additional difficulties associated with attachment.

The candidate materials considered for impurity control are listed in Table 2. These materials were selected from a larger pool of possible materials based upon the properties requirements given in Table 1. The plasma side materials are divided into low-Z, medium-Z, and high-Z materials. At low plasma edge temperatures ($\lesssim$ 50 eV) all materials may be used, but high-Z materials, as will be described, are predicted to yield the greatest lifetimes. At higher edge temperatures, both medium and high-Z materials are unacceptable due to excessive self sputtering. The permissible plasma side materials are those whose self sputtering coefficients never exceed unity, which limits the selection to materials whose atomic weights are at or below the atomic weight of SiC. The candidate heat sink materials are copper alloys and transition metal alloys.

The materials information presented in the following sections is taken largely from the recent FED/INTOR critical issues study.[1] The materials assessment for this study included

0022-3115/84/$03.00

Table 1. Desirable Characteristics of Impurity Control Materials

Property	Desirable Value	Purpose
Thermal conductivity	High	Minimize thermal stress
Thermal expansion	Low	
Young's modulus	Low	
Specific heat	High	Minimize effect of thermal shock
Yield strength	High	Maximize allowable stress
Ultimate tensile strength	High	
Uniform elongation	High	Maximize ability to withstand off-normal events
Total elongation	High	
Swelling	Low	Minimize dimensional and physical property changes
Creep	Low	Minimize dimensional changes
Fatigue	Low	Prevent catastrophic failure
Crack growth	Low	
Corrosion	Low	Prevent wall thinning and coolant channel plugging
Stress corrosion cracking	Low	Prevent catastrophic failure
Transmutations	Low	Prevent alloy compositional change
Sputtering	Low	Reduce wall thinning and plasma impurities

Table 2. Candidate Impurity Control Materials

Plasma-Side Materials	
	Low-Z: C, Be, B, TiC, SiC, B_4C, BeO
	Med.-Z: Stainless Steel, V
	High-Z: W, Ta, Nb
Heat Sink Materials	
	Copper Alloy
	Vanadium Alloy
	Niobium Alloy

contributions from experts around the U.S. in the areas of sputtering, hydrogen and helium retention and release, bulk properties, irradiation effects, and fabrication.

2. SPUTTERING

2.1 Physical sputtering

Physical sputtering has been extensively reviewed previously, and many of the experimental results are available in two compilations.[2,3] The data for light ion sputterring are fairly complete for energies up to 10 keV. Self-sputtering data are available for a limited number of targets and considerable reliance on extrapolations from inert gas sputtering is required.

For Be, the measured yields compare very well with yields for BeO[3] and are probably more representative of the oxide surface. Physical sputtering of graphite is similar to that of Be. Self-sputtering yields are generally much larger than light ion yields and can lead to catastrophic increases in impurity introduction if they exceed unity. Self-sputtering yields of less than unity are expected for the lighter targets, Be, B, C, and probably SiC at all energies. Self-sputtering yields exceed unity in V, stainless steel, Mo and W for energies above 0.6 - 1 keV. Qualitative estimates of the accuracy of the data range from ± 30% for light ions in stainless steel to factors of 2-4 in some self-ion cases. The data are more reliable near the peaks in the sputtering curves where the yields are larger and less energy dependent.

Surfaces exposed to significant impurity fluxes (such as limiters and divertor plates) will necessarily accumulate redeposited material since sputtering yields greater than unity cannot be tolerated. All surfaces are possible candidates for hydrocarbon and oxide contamination which can also significantly affect sputtering yields. Surface conditions probably represent the largest uncertainty in predicting sputtering yields in fusion devices.

There is considerable evidence[4,5] that sputter-deposited material exhibits similar

sputtering behavior as bulk material of the same composition. Redeposited plasma-side material is also expected to incorporate significant concentrations of H isotopes and He. High fluence sputtering experiments are routinely performed on projectile-saturated surfaces, and H and He loading probably reduces bulk yields by less than a factor of two. These effects are already incorporated in the data base.

Surface morphology can also affect sputtering yields. Roughened surfaces often show slightly higher yields than polished surfaces,[2] but with severe roughening as represented by honeycomb or matted fiber surfaces decreases yields by factors of 2-6.[6,7] The sputtering yield is particularly sensitive to surface morphology at glancing angles of incidence.

2.2 Chemical sputtering

Chemical sputtering of graphite by light ion bombardment has been discussed and reviewed in the past.[8-17] Most investigations have focused on the formation of methane which occurs in the temperature range between 200° and 800°C. The maximum production rate has been shown to occur around 1 keV incident hydrogen energy and at a temperature of about 550°-600°C.[18] The energy and temperature dependences of chemical sputtering are shown to be essentially independent of the various forms of carbon. These conclusions are in agreement with the earlier results of Roth, et al.,[13] and Smith and Meyer.[15] Results of other works[16,17] yield a maximum for CH_4 production at about 800°C. It seems that the variations in the results are due to experimental errors as well as to using different types of graphite surfaces.

In recent work, Roth, et al.[19] studies graphite erosion by H^+, D^+ and He^+ above 1000 K. Figure 1 (taken from Ref. 19) shows the sputtering yield of carbon as a function of temperature for 1 keV H^+ and D^+ incident energy ions and for 3 keV He^+ ions. The sputtering yield of carbon bombarded by H^+ and D^+ ions increases with

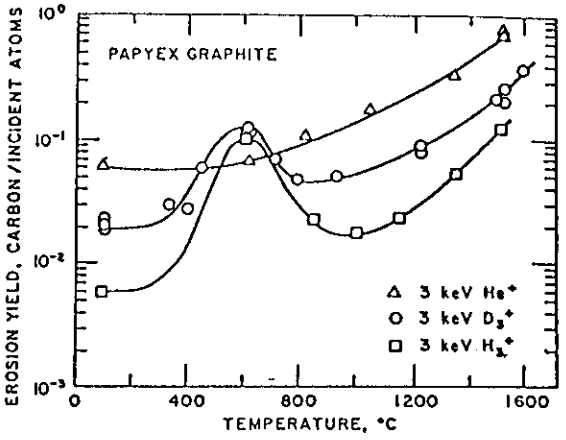

FIGURE 1
Temperature dependence of the chemical sputtering yield of papyex graphite.

increasing temperature reaching a maximum at about 525°C corresponding to the maximum in methane production. As the temperature is raised beyond 525°C, the erosion rate decreases, but above ~ 1000°C, erosion again rapidly increases with no apparent peak. On the other hand, helium bombardment does not produce an erosion peak at 525°C, but does cause a rapid rise in sputtering above 700°C. High erosion rates above 1000°C indicate a mechanism other than physical or chemical sputtering, since no hydrocarbon formation was detected at the high temperatures.[19]

In the chemical sputtering of B_4C, SiC, and TiC, the erosion yield effects are much smaller than those observed in the case of graphite. For B_4C and SiC surfaces bombarded by thermal atomic hydrogen beams, methane production is observed initially but falls to a low level due to the depletion of carbon atoms in the surface layer.[20] For energetic H^+ bombardment of B_4C at 20 keV, a temperature dependence of methane production is observed, peaking at 200°C; but it is an order of magnitude smaller than the methane production from graphite, given the same conditions.[21] Data on SiC indicates a broad temperature peak of 500°-650°C, having a chemical erosion yield two times greater than the physical sputtering yield for energetic hydrogen.[10-12]

Titanium carbide which has been used as a coating on graphite limiters in ISX-A showed less of the plasma contamination problems associated with the use of graphite alone.[22] Thus, based upon the sparse data available, one may conclude that the chemical erosion enhancement of carbides is within a factor of two uncertainty of the physical sputtering yield for most temperatures and does not present the same severe impurity problems as graphite. More work is needed in the area of chemical sputtering $\geq$ 1000°C where surface segregation effects become important.

2.3 Neutron irradiation effects

Older reviews of irradiation effects in beryllium[23,24] based on relatively low fluence experimental results, conclude that the metal is intrinsically resistant to purely displacement damage events, and that observed effects of irradiation at temperatures above the cryogenic range are due primarily to transmutation helium, rather than to point defects or defect clusters. Measurements of resistivity[25,26] and thermal conductivity[26] in material irradiated at 20 or 77 K showed that recovery was complete, with no residual damage on annealing to 270 K. More direct evidence was developed by Carpenter and Fleck[27] using high-energy electron bombardment and direct TEM observation of the damage microstructure. They found that, although visible damage resulted in bombardments near room temperature, no visible damage could be developed for bombardments producing 15 dpa at 300°C.

Few data are available on the swelling produced by high fluence, elevated-temperature irradiation. Figure 2 shows the swelling that can result when helium-containing material is annealed at temperatures well above the irradiation temperatures. These results suggest that high swelling values can be expected if temperatures much above 700°C are allowed.

The degradation in Be mechanical properties that results from the elevated-temperature irradiation of beryllium is produced by the combination of matrix hardening that results from bubble pinning of dislocations and the grain boundary weakening that results from helium accumulation at the boundary. Representative mechanical properties of irradiated material, taken from the review of Bush[23] are shown in Fig. 3. The considerable data collected in Fig. 3 show a decreasing elongation with increasing fluence as a general theme of the many collected conditions.

The use of BeO in fission reactor components has mainly been limited by the tendency of the material to develop microcracks, with an attendant loss of properties, at quite low neutron fluences. The cause of this cracking, for irradiation at temperatures below about 700°C, is the anisotropic expansion of the hexagonal crystal lattice. The swelling due to lattice distortion and microcracking is a consequence of the displacement damage process, and any effect of helium production in (n,α) reactions is secondary. The predicted swelling curves based on the measured data are shown in Fig. 4.[28] Figure 4 also includes predictions of a flux effect on swelling that is relatively unimportant for temperatures below about 700°C.

At higher temperatures the helium produced in transmutation reactions is believed to be important in determining the swelling behavior. Swelling of BeO for high fluence, high temperature irradiation is available only in a single, unpublished data set. Hurley and Clinard[29,30] irradiated two grades of beryllium oxide at temperatures between 650° and 825°C, to fast reactor fluences up to 2.2×10^{26} n/m^2, and found swelling up to 11%.

Thermal conductivity of BeO is significantly affected by neutron irradiation throughout the full range of temperatures for which it has been measured. Extrapolated low fluence data are shown in Fig. 5. This model shows a decrease in conductivity with increasing fluence, with the

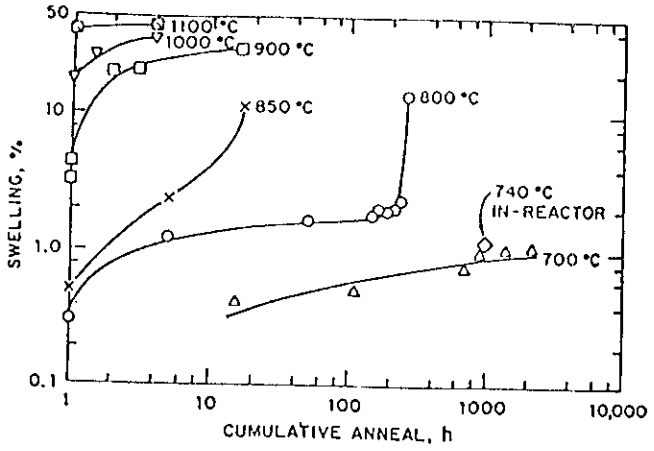

FIGURE 2
The effect of time and temperature on the swelling of irradiated beryllium.

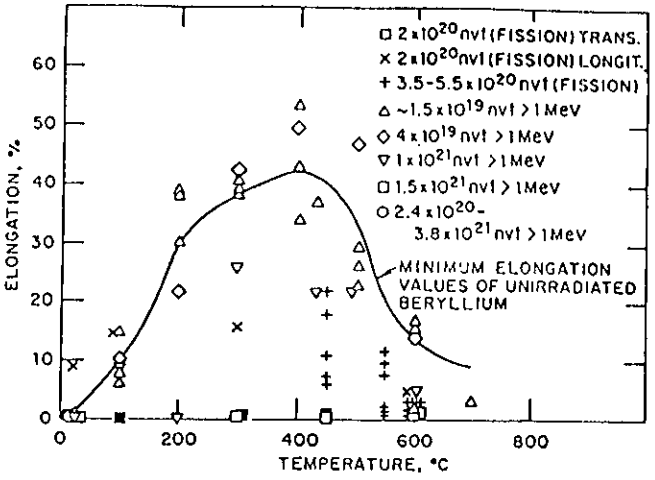

FIGURE 3
The influence of irradiation and tensile testing temperature on the elongation of beryllium.

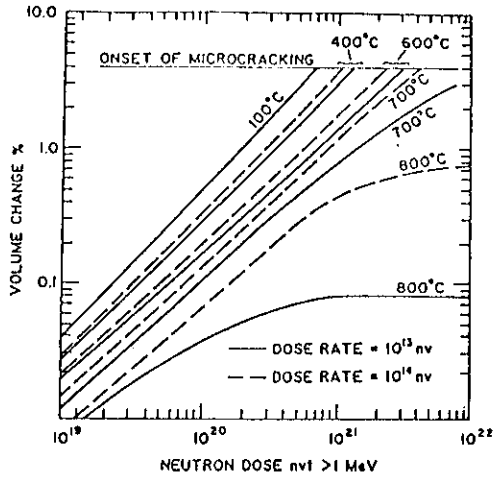

FIGURE 4
Predicted volume expansion of BeO as a function of dose, dose rate, and temperature.

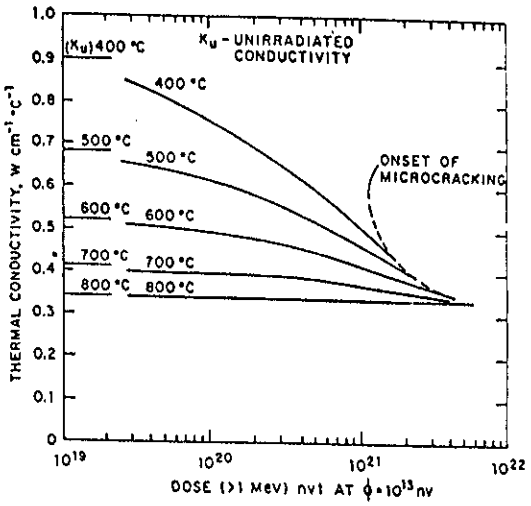

FIGURE 5
Extrapolated values for the thermal conductivity of BeO as a function of dose and irradiation temperature for a dose rate of 10^{13} nv.

rate of change decreasing as the irradiation temperature is increased. Little effect is predicted for irradiation at 800°C or higher.

The microcracking that occurs during irradiation of BeO leads to a severe degradation in other properties. In particular, the internal cracks signal a loss of strength. A precipitous drop of the modulus of rupture is predicted at the fluence at which microcracking occurs.[31] Microcracking, then, can be taken as the signal for the end of useful life for BeO structural component service.

A typical set of swelling design curves for an isotropic nuclear graphite is given in Fig. 6. The classic definition of lifetime is that point in time (fluence) when the graphite distortion returns to its original volume. In actual fact, the mechanical strength persists for some time after this point. The generally expected changes in thermophysical and mechanical properties that will result from irradiation at ~ 500°C are summarized in Table 3.[1]

The swelling of silicon carbide produced by irradiation can be divided into two temperature regimes. For irradiation at temperatures below about 1000°C, irradiation causes a lattice expansion that saturates at relatively low

Table 3. Extrapolated Property Values for Irradiatied GraphNOL N3M

Property	Generalized Behavior	Numerical Values
Thermal conductivity	Monotonic exponential decrease, saturating at about half-life.	Saturates at about 30 W/(m.K).
Thermal expansion	Rapid rise and fall within first third of life.	Maximum at perhaps 50% over initial value. Saturates at about 75% of initial value.
Tensile strength	Linear falloff with fluence.	About 50% of initial value at end-of-life.
Strain-to-failure	Gradual falloff saturating at about half-life.	Saturates at about 40% of initial value.
Moduli (Young's and shear)	Gradual increase, saturating at about half-life.	Saturates at 2.5.3 times initial value.
Radiation creep	No information; appears to be relatively insensitive to graphite grade.	Assume behaves as other nuclear graphites.

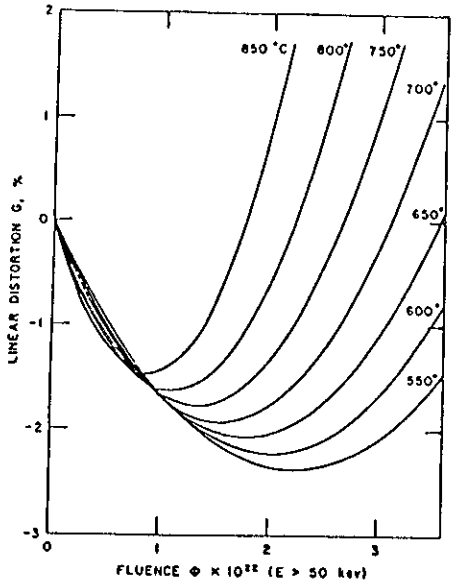

FIGURE 6
Typical graphite design curves for a nuclear reactor. Graphite is assumed isotropic.

fluences. The resulting swelling is temperature dependent, with the saturation volume falling from about 3% at room temperature to near 0.3% at 1000°C. For irradiation at higher temperatures, voids form (as in the case in metals) and higher swelling levels are projected at higher fluences. Hopkins, et al.[32] predict that at irradiation temperatures above about 1300 K void swelling will limit the useful lifetime to fluences of a few x 10^{26} n/m^2.

The thermophysical property most severely affected by irradiation is the thermal conductivity. The conductivity is plotted in Fig. 7. This shows the severe reduction in conductivity, produced even by low-fluence exposures (~ 10^{25} n/m^2). Figure 7 also shows that while there is a very strong dependence of the thermal conductivity on the form of the SiC, for unirradiated material, the conductivity of self-bonded and pyrolytic material are essentially equivalent after irradiation. Therefore, regardless of the prospects of developing a high conductivity grade of SiC, it is likely that the degraded value after service to modest irradiation fluence will be independent of the starting value.

Interest in tungsten for nuclear reactor applications has been very limited; hence, the data base is very sparse. The highest fluence data are those reported by Steichen[33] for EBR-II irradiations at ~ 385°C (658 K). Tensile specimens of sheet material which had been stress-relieved at 1273 K for 1/2 hour to a reported grain size of 5 to 7 μm were irradiated to fluence levels of 0.4 and 0.9 x 10^{26} n/m^2 (E > 0.1 MeV). Post-irradiation tensile tests, conducted in the range 295 to 1200 K, indicated

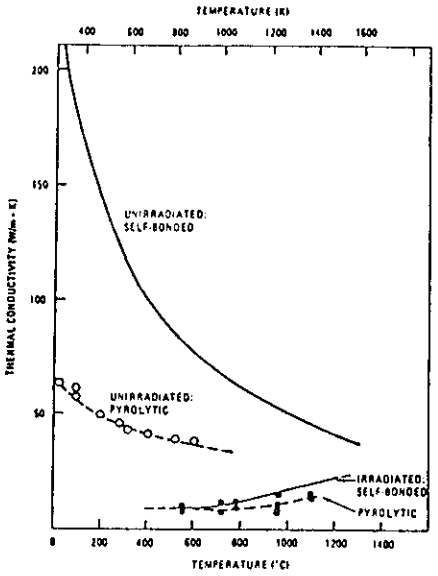

FIGURE 7
Thermal conductivity of unirradiated SiC and irradiated SiC at the irradiation temperature as a function of temperature (fluences between 10^{25} and 10^{26} n/m^2).

the tensile yield strength was approximately doubled by irradiation over the full temperature range. The ductile-brittle transition temperature, as measured or observed by values of the tensile ductility (i.e., percent elongation or reduction in area), was raised from an initial value of ~ 65°C to ~ 230°C by the irradiation.

3. HEAT SINK MATERIALS

Two classes of alloys, copper alloys and refractory metal alloys, have been considered Copper alloys were selected because of their high thermal conductivity and their availability. Refractory metal alloys, as typified by V-15Cr-5Ti, have higher temperature capability, acceptable thermal conductivity, and good resistance to radiation damage. They are not, however, readily available.

3.1 Thermophysical properties

The temperature dependent thermophysical properties of V-15Cr-5Ti are shown in Table 4.[34-37] Both the specific heat and electrical resistivity values are those of pure vanadium.[34-37] The elastic modulus values are those

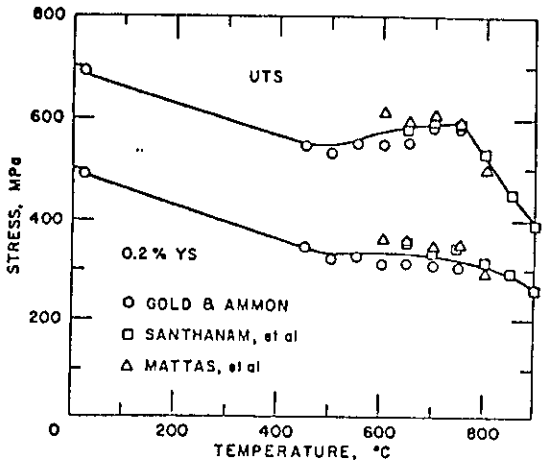

FIGURE 8
Tensile properties of V-15Cr-5Ti.

of a V-15Ti-7.5Cr alloy. The temperature dependent thermophysical properties of several copper alloys are shown in Table 5.[34,37-40] The copper alloys have superior thermal conductivity values, but they also have significantly larger values for thermal expansion compared with the vanadium alloy.

3.2 Mechanical properties

The tensile strength of V-15Cr-5Ti is shown in Fig. 8.[41-43] Both the ultimate strength and the 0.2% yield strength are approximately independent of temperature in the range from 450-750°C. Above this point, the strength begins to drop off, but reasonable strength remains up to 900°C. The uniform elongation of this alloy is approximately 23% at room temperature, and it is in the range of 11-16% from 450 to 800°C.

The 0.2% yield strength for 50% cold-worked OFHC copper, AMAX-MZC in the 40% cold-worked and aged condition, and the copper-beryllium (Cu-Be) alloys in the annealed and heat treated conditions are compared in Fig. 9.[38-40,44,45] The strength begins to decrease at ~ 225°C (498 K) for OFHC copper and at ~ 400°C (673 K) for Cu-Be alloys. The effect of alloying is to increase the strength, but generally at the expense of the thermal conductivity as shown in Table 5.

The room temperature fatigue behavior of V-15Cr-5Ti and pure copper are compared in

Table 4. Thermophysical Properties of Vanadium and Vanadium Alloys

Temperature °K	Mean Thermal Expansion x10^{-6}/K	Thermal Cond. (W/mK)	Specific Ht. (J/kgK)	Elastic Mod. (GPa)	Electrical Res. (μΩ-cm)
273	9.3	21.3	451	127	26.0
373	9.5	22.7	473	126	32.1
473	9.7	24.0	494	124	38.2
573	10.0	25.4	516	122	44.3
673	10.2	26.7	537	120	50.4
773	10.4	28.1	558	118	56.6
873	10.6	29.4	580	116	62.7

Table 5. Thermophysical Properties of Copper Alloys

Alloy	Temp. (K)	Thermal Exp. x10^{-6}/K	Resistivity μΩ-cm	Thermal Cond. W/mK	Elastic Modulus GPa	Spec. Ht. J/KgK
OHFC	300	16.7	1.6	391	121	385
	500	17.3	3.0	380		
	700	18.0	4.6	370		
AMAX-MZC	300	16.0	2.2	322	138	393
0.1 Zr,0.6 Cr	500	18.4				
0.05 Mg	700	20.0				
Alloy 25	300	16.5	7.7	117	125	418
Cu-1.85 Be	500	17.0		135	116	422
0.25 Co+Ni	700			148		
Alloy 10	300		3.79	230	121	418
0.5 Be	500	17.6		244	103	
2.5 Co or Ni	700			270	89	

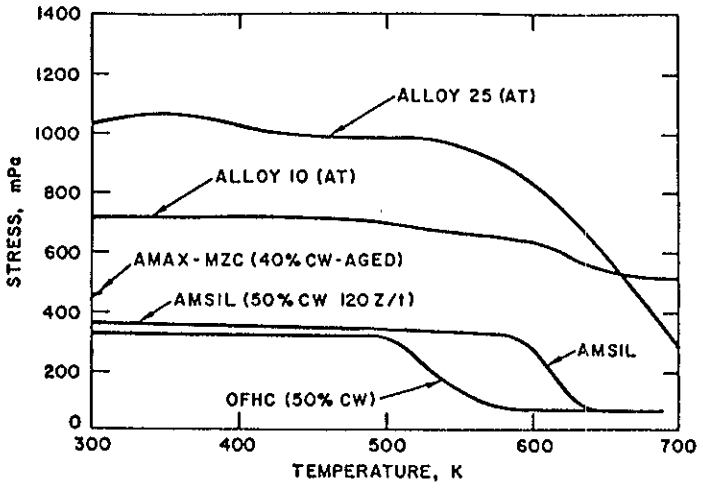

FIGURE 9
Yield strength as a function of temperature for candidate copper alloys.

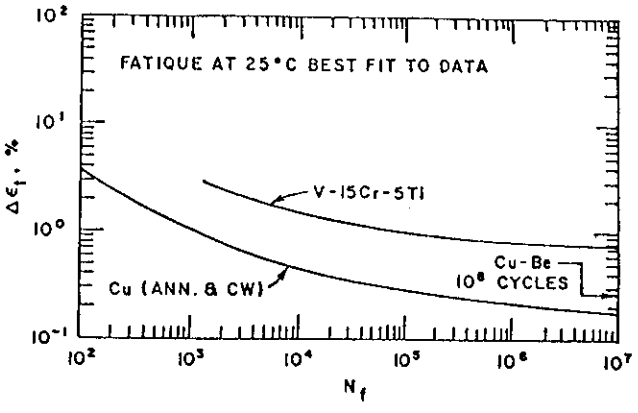

FIGURE 10
Fatigue data for copper and vanadium alloys at room temperature.

Fig. 10.[46,47] The V-15Cr-5Ti exhibits superior fatigue behavior with an endurance limit of ~ 0.8%, compared with ~ 0.15% for pure copper. Cu-Be alloys exhibit improved fatigue behavior over pure copper in the high cycle range, but they are still considerably inferior to V-15Cr-5Ti.

3.3 Radiation effects

The temperature dependence for void swelling of the V-15Cr-5Ti alloy, commercial grade vanadium, and 6-pass zone refined vanadium has been determined for neutron irradiation to 3.6×10^{26} neutrons/m^2 (E > 0.1 MeV). In contrast to the zone refined and commercial vanadium, the V-15Cr-5Ti alloy shows essentially no void swelling following irradiation at 450 - 600°C.[48-50] The unalloyed vanadium shows a peak swelling of ~ 1% at ~ 525°C. In the case of the ternary alloys, both V-15Cr-5Ti and V-15Ti-7.5Cr alloys were irradiated at 425°C to a damage of ~ 14 dpa without the formation of voids.[49] Irradiation at 600°C resulted in some void formation in both alloys, but the total swelling was negligible. In another experiment, V-15Cr-5Ti was irradiated to ~ 20 dpa at 450, 550, and 600°C.[51] Except for a few isolated voids at 550°C, there was no tendency for void formation or swelling. In a recent experiment, helium was injected into V-20Ti samples in concentrations of 90 and 900 appm prior to irradiation to 17 dpa at temperatures of 400, 575, 625 and 700°C.[52] Numerous cavities were observed in the samples following irradiation, but the total swelling in all cases was negligible.

The effect of radiation on the tensile properties can be divided into three regimes: low temperatures ($T \leq 100$°C), intermediate temperatures ($300° \leq T \leq 650$°C), and high temperatures ($T \geq 650$°C). Vanadium alloys which are irradiated and tested at low temperatures generally exhibit rapid embrittlement due to plastic instability.[53] The reduction of uniform elongation to nearly zero by the early onset of plastic instability in irradiated bcc metals and alloys has been observed in a number of systems.[54,55] Plastic instability has been observed at fluence levels as low as 0.0095 dpa, where the uniform elongation was close to zero while the total elongation was ~ 8%. At the highest fluence level of ~ 1 dpa, the total elongation remained above 2% and the fracture mode was fully ductile. There was no indication that the irradiation hardening has saturated at this damage level.

At intermediate temperatures, the influence on the tensile properties is far less severe than at low temperatures. V-20Ti alloys which were irradiated up to ~ 18 dpa at temperatures of 500-600°C exhibited some irradiation hardening, but the uniform and total elongation was little affected up to test temperatures of ~ 700°C.[49] In another series of tests, V-20Ti was irradiated to ~ 36 dpa at temperatures ranging from 370°-900°C.[56] Tensile tests in the range of 600°-750°C showed similar behavior.

At high temperatures, the ductility of vanadium alloys will decrease due to the onset of helium embrittlement. In the case of V-15Cr-5Ti, helium embrittlmenet has been studied in samples where helium was introduced by ion injection and by tritium decay.[42,43] Injected samples which contained 25 appm He exhibited embrittlement at temperatures $\geq$ 750°C, whereas the tritium decay samples containing 35 appm He exhibited embrittlement at temperatures $\geq$ 700°C. A recent experiment examined the combined effects of helium pre-injection followed by neutron irradiation to ~ 17 dpa in V-20Ti.[52] Samples containing 90 and 200 appm showed no loss of ductility at 575°C, but showed marked ductility loss at ~ 700°C (3% uniform elongation). It should be pointed out that even where the loss of ductility was large, the uniform elongation remained above 1% in all of these experiments, even up to test temperatures of 900°C.

The swelling of pure copper due to the accumulation of irradiation-produced defects in voids during neutron irradiation is shown as a function of irradiation temperature in Fig. 11.[57-59] The void swelling of copper is minimal for irradiation temperatures less than ~ 200°C or greater than ~ 450°C.[57] The swelling of copper after neutron irradiation to a fluence of 5 x 10^{24} neutrons/m^2 (E > 0.1 MeV) has a peak value of ~ 0.5% at ~ 330°C.[58]

The effect of substitutional alloying elements on the void swelling of copper during neutron irradiation have been studied.[59,60] Alloying copper with 1-3 a/o aluminum, germanium, silicon or nickel can result in a significant reduction of the void swelling of copper. The swelling of copper is increased by 1.0 a/o additions of silver or cadmium on 1 MeV electron irradiation at 250°C.[61] However, the alloying of copper with 1.2 a/o beryllium results in no void formation at 250°C on electron irradiation to 100 dpa.[61] The irradiation of copper containing 1.35 a/o beryllium at 327-397°C with 300 keV Cu^+ ions to 8 dpa results in the formation of very fine precipitates and no voids.[62]

The dependence of room-temperature yield strength, tensile strength, percent elongation, and reduction in cross-sectional area of copper on neutron fluence (E > 2.8 MeV) following irradiation at 80°C is shown in Fig. 12.[63] The experimental data show that the yield stress of copper is greatly increased by neutron irradiation with the rate of increase diminishing as the neutron fluence increases. The total elongation is reduced significantly by irradiation for fluences up to at least 10^{24} neutrons/m^2. The reduction in area at fracture also tends to decrease with irradiation but only by a small amount.

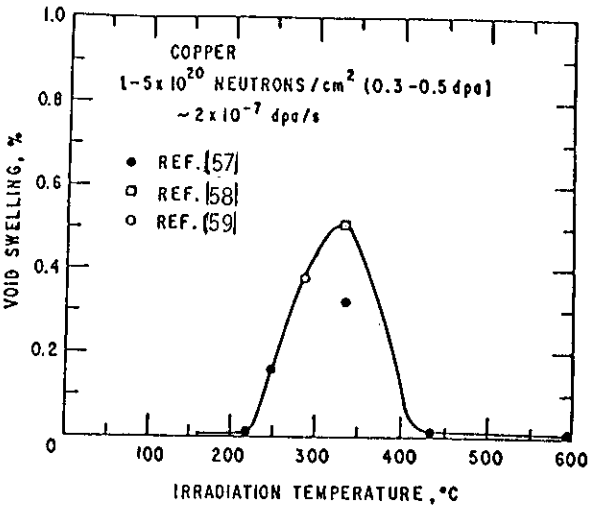

FIGURE 11
Dependence of void swelling of neutron-irradiated copper on temperature.

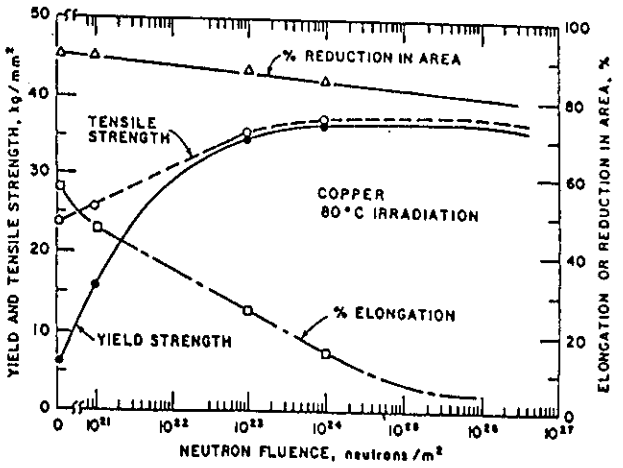

FIGURE 12
Effect of irradiation at 80°C on room-temperature tensile properties of copper.

4. DESIGN IMPLICATIONS

4.1 Plasma edge considerations

The selection of materials depends upon the energies of particles at the plasma edge. Presently, it is envisioned that particles sputtered from impurity control surfaces enter the plasma edge where they are ionized. In the ionized state, it is expected that they will follow magnetic field lines back to the surface to cause additional sputtering. The sputtering coefficient is a function of the particle energy which depends on the ionization state and the magnitude of the sheath potential. Calculations

indicate that the ionization state of sputtered particles is likely to be 3-4 in tokamaks, and the magnitude of the sheath potential is ~ 3 T_e, giving a total energy to the returning particle of 9-12 T_e.[1] A key conclusion of the design studies is that a self-sputtering cascade is predicted when the self-sputtering coefficient exceeds unity. Thus, the self sputtering should always remain below unity for a workable impurity control system.

These considerations place severe restrictions on the selection of plasma side materials. Medium and high-Z materials, where the self-sputtering coefficient exceeds one at energies of 0.6-1.0 keV, may only be used at plasma edge temperatures $\lesssim$ 50 eV. Only low-Z materials, whose self-sputtering coefficients never exceed unity, can be used at higher energies. For convenience, three different plasma edge regimes have been considered.

1) Edge temperatures above 700 eV could reduce the erosion of low-Z materials. The high edge energies are above the peak in the sputtering curves, and the particle flux is reduced as the edge temperature increases. Unfortunately, it is unlikely that these high edge temperatures can be achieved in practice.

2) At medium edge temperatures (100 eV < T_e < 400 eV) only low-Z materials can be used because of self-sputtering considerations. However, erosion is expected to be severe in this regime, leading to short component lifetimes.

3) Edge temperatures $\lesssim$ 50 eV allow the use of high-Z materials and low net sputtering rates. This is the most attractive engineering regime, but it is not known if these conditions can be achieved in practice.

4.2 Erosion/redeposition

Detailed calculations of the rates of erosion and concomitant redeposition at impurity control surfaces were made using the REDEP code.[64] The code incorporates the physical sputtering behavior of materials described in Section 2.1 along with a model of the plasma edge. A typical example of the calculations is shown in Fig. 13 for the INTOR limiter at a plasma edge temperature of 100 eV. Beryllium is the surface material. The total erosion and redeposition rates are predicted to be 100-160 cm/y. However, the net erosion rate is predicted to be only 1-5 cm/y on the front surface. The leading edges are predicted to have net erosion rates of 29 cm/y. The high loss rate of material is disturbing, and this issue deserves additional experimental and theoretical effort.

4.3 Component lifetime

The prediction of component lifetime should incorporate sputtering and disruption losses, estimates of the maximum allowable thickness of the plasma side materials, mechanical property limits for the heat sink material, and the influence of radiation on bulk properties. The maximum allowable thicknesses are determined by temperature and stress limitations. The most important mechanical property limitation for high cycle machines is fatigue cracking. The influence of radiation is often poorly understood for these materials, and further work is required to thoroughly evaluate irradiation effects.

Figure 14 illustrates the lifetime determination for the INTOR limiter leading edge with a plasma edge temperature of 700 eV.[1] Beryllium is the surface material and V-15Cr-5Ti is the heat sink material. The graph indicates that erosion lifetime will increase linearly with the plasma side thickness. The Be temperature limit and stress limit restricts the thickness to 2.6 and 2.9 cm respectively. The fatigue lifetime decreases rapidly with increasing thickness, and it crosses the erosion lifetime curve at ~ 2.5 cm. The estimated lifetime is only ~ 1 y.

5. MAJOR UNCERTAINTIES

The major uncertainites for impurity control materials are in the areas of: 1) physical

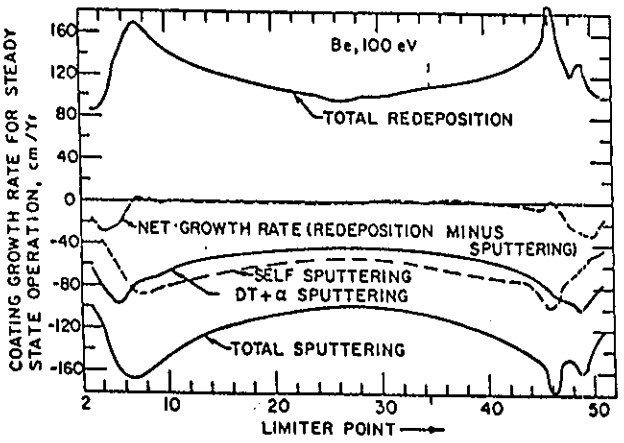

FIGURE 13
Erosion (physical sputtering only) and redeposition rates for beryllium as a function of spatial points at the limiter surface for a plasma-edge temperature of 100 eV.

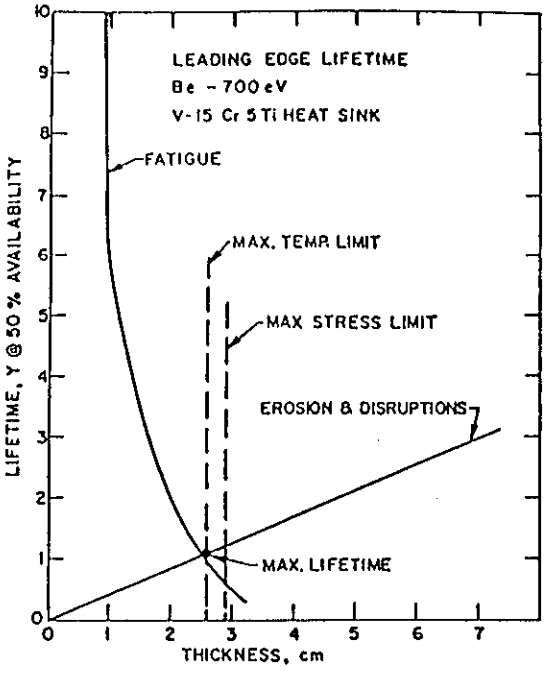

FIGURE 14
Effect of surface material thickness on Be limiter leading edge.

sputtering, 2) erosion/redeposition, 3) disruptions, 4) irradiation effects, 5) fatigue/crack propagation, and 6) tile/heat sink interface.

The lifetimes of impurity control components are sensitive to the values for the physical sputtering coefficients of plasma side materials. The areas of greatest uncertainties are the sputtering coefficients due to tritium ions, self sputtering yields, particularly the energy at which self sputtering exceeds unity for medium and high-Z materials, and the sputtering coefficients for highly irregular and redeposited surfaces. No laboratory data exists for tritium sputtering, and the predicted sputtering coefficients are expected to be accurate to only within a factor of two.

The lifetimes are also very dependent on high redeposition rates for sputtered particles. Such high redeposition rates have been predicted by computer models, but there are no data to confirm these calculations. Substantial improvement in modeling of erosion/redeposition is required and improvement in the data base for such calculations is necessary.

Disruptions could have a large influence on the operation of the impurity control and first wall system because of potentially large vaporization and melt layer losses. The degree of material loss depends on the frequency, energy density, and duration of the disruptions. In addition, the melt layer losses will depend on the accompanying magnetic and mechanical forces during the disruptions. All of these quantities are uncertain at this time.

The bulk mechanical property data base for both the plasma side and heat sink materials is small, and therefore the response of these materials to the heat and irradiation conditions in advanced fusion devices cannot be predicted with certainty. Also, the duplex structure required for impurity control components introduces the need for an interface bond whose properties have yet to be determined. The properties of greatest concern are the fatigue/crack propagation properties and the effects of irradiation on swelling and embrittlement of the materials.

ACKNOWLEDGEMENT

The authors wish to acknowledge the individuals who participated in the FED/INTOR

study. They are: M. Baskes, J. Davis, J. Draly, R. Domagala, R. Gold, D. Gruen, J. Klinger, B. Loomis, H. Mantz, D. Mattox, A. Mullendore, J. Roberto, K. Sankaran, F. W. Wiffen and K. Wilson. Work supported by U.S. Department of Energy.

REFERENCES

1. M. A. Abdou, et al., "Impurity Control and First Wall Engineering," FED/INTOR/ICFW/82-17.

2. H. H. Anderson and H. L. Bay, in Sputtering by Particle Bombardment I, edited by R. Behrisch, Springer-Verlag (1981); J. Nucl. Mater. 93-94 (1980) 625.

3. J. Roth, J. Bohdansky, and W. Ottenberger, MPI fur Plasmaphysik Report IPP 9/26, Garching, (1979).

4. H. Von Seefeld, H. Schmidl, R. Behrisch, and B. M. U. Scherzer, J. Nucl. Mater. 63 (1976) 215.

5. J. B. Roberto, R. A. Zuhr, J. L. Moore, and G. D. Alton, J. Nucl. Mater. 85-86 (1979) 1073.

6. S. N. Cramer, and E. M. Oblow, Nucl. Fus. 16, (1976) 158.

7. P. J. Gierszewski, N. E. Todreas, B. Mikic, and T. F. Yang, MIT Plasma Fusion Center Report PFC/RR-81-20, Cambridge, Mass. (1981).

8. C. I. H. Ashby, Sandia Laboratories Technical Report, SAND810803, (1981).

9. N. P. Busharov, E. A. Gorbatov, V. M. Gusev, M. I. Guseva, and Yu. V. Martynenko, J. Nucl. Mater. 63 (1976) 230.

10. J. Bohdansky, H. L. Bay, and W. Ottenberger, J. Nucl. Mater. 76&77 (1978) 163.

11. J. A. Borders, R. A. Langley, and K. L. Wilson, J. Nucl. Mater. 76&77 (1978) 168.

12. R. A. Langley, R. S. Blewer, and J. Roth, J. Nucl. Mater. 76&77 (1978) 313.

13. J. Roth, J. Bohdansky, W. Poschenrieder, and M. K. Sinha, J. Nucl. Mater. 63 (1976) 222.

14. J. N. Smith, Jr., C. H. Meyer, and J. K. Layton, J. Nucl. Mater. 67 (1977) 234.

15. J. N. Smith, Jr. and C. H. Meyer, Jr., J. Nucl. Mater. 76 & 77 (1978) 193.

16. S. K. Erents, C. M. Braganza and G. M. McCracken, J. Nucl. Mater. 63 (1976) 399.

17. C. M. Braganza, S. K. Erents, and G. M. McCracken, J. Nucl. Mater. 76 & 77 (1978) 204.

18. R. Yamada, K. Nakamura, K. Sone, and M. Saidoh, J. Nucl. Mater. 95 (1980) 278.

19. J. Roth, J. Bohdansky, and K. L. Wilson, J. Nucl. Mater. 111 & 112 (1982) 775.

20. S. Veprek, M. R. Haque, and H. R. Oswald, J. Nucl. Mater. 63 (1976) 405.

21. G. M. McCracken, and P. E. Stott, Nuclear Fusion 19 (1979) 889.

22. J. B. Whitley and H. W. Mullendore, Thin Solid Films 73 (1980) 81.

23. S. H. Bush, Irradiation Effects in Cladding and Structural Materials, American Society for Metals (1965).

24. M. Kangilaski, Radiation Effects Design Handbook, Section 7, Structural Alloys, NASA CR-1873 (1971).

25. T. H. Blewitt, ORNL-2614 (1958) 64.

26. J. M. Williams, N. E. Hinkle, and W. P. Eatherly, ORNL/TM-3917 (1972).

27. G. J. C. Carpenter and R. G. Fleck, "Electron Irradiation Damage in Beryllium in a High Voltage Electron Microscope," Paper 26 in Beryllium 1977.

28. R. S. Wilks, J. Nucl. Mater. 26 (1968) 137.

29. G. F. Hurley and F. W. Clinard, Jr., in Special Purpose Materials Annual Progress Report, DOE/ET-0095 (1975) 59.

30. G. F. Hurley, Personal communication on swelling in irradiated BeO (1982).

31. B. S. Hickman, "Radiation Effects in Beryllium and Beryllium Oxide," in Studies in Radiation Effects, Series A: Physical and Chemical, Vol. 1 (ed. by G. J. Dienes), Gordon and Breach, New York (1966) 72.

32. G. R. Hopkins, et al., "Carbon and Silicon Carbide as Frist Wall Materials in Inertical Confinement Fusion Reactors," GA-A14894, General Atomic Company (1978).

33. J. M. Steichen, Nucl. Mater., 60 (1976) 13.

34. Y. S. Touloukian, ed., "Thermophysical Properties of High Temperature Solid Materials," The MacMillan Company, New York (1967).

35. R. E. Gold, et al., "The Technical Assessment of Vanadium Base Alloys for Fusion Reactor Applications," COO-4540-1 (Vol. 2) (1978).

36. F. L. Yaggee, E. R. Gilberts, and J. W. Stiles, J. Less Common Metals, 19 (1969) 39.

37. W. D. Wilkinson, "Properties of Refractory Metals," Gordon and Breach Science Publishers, New York (1969).

38. Metals Handbook, Ninth Edition, Vol. 2, American Society for Metals, Metals Park, Ohio (1979).

39. "Berylco Alloys, A Guide to Their Selection and Use," Cabot Berylco Bulletin 106 PDl (1982).

40. "AMAX-MZC Copper, Oxygen-Free Copper, Plus Magnesium, Zirconium, and Chromium AMAX Copper, Inc. Bulletin.

41. R. E. Gold and R. L. Ammon, ADIP Quarterly Progress Report, DOE/ER-0045/6, (1981) 96.

42. R. F. Mattas, H. Wiedersich, D. G. Atteridge, A. B. Johnson, and J. F. Remark, Proc. of the 2nd Topical Mtg. on the Tech. of Controlled Nucl. Fusion, CONF-760935-P1, Vol. 1. (1977) 199.

43. A. T. Santhanam, A. Taylor, and S. D. Harkness, Nucl. Mater., 18 (1973) 302.

44. D. L. Harrod, E. Vandergrift and L. France, "Mechanical Property Determinaton of High Conductivity Metals and Alloys - Final Report," Westinghouse Astronuclear Laboratory, WANL-M-FR-72-005 (1973).

45. K. G. Wilke, "ASK Product Concept Applied to Copper-Beryllium Alloys," Metallurgical Report No. M-44, Kawecki Berylco Industries, Inc. (1965).

46. R. E. Gold, ADIP Semiannual Progress Report, DOE/ER/0045/7 (1981) 122.

47. M. C. Murphy, Fatigue of Engineering Matls. and Structures, 4, (1981) 199.

48. A. F. Bartlett, J. H. Evans, B. L. Eyre, E. A. Terry, and T. M. Williams, "Proc. Intl. Conf. on Radiation Effects and Tritium Technology for Fusion Reactors, Vol. I, (1976) 122.

49. R. Carlander, S. D. Harkness, and A. T. Santhanam, "Effects of Radiation on Substructure and Mechanical Properties of Metals and Alloys, "ASTM-STP 529, American Society for Testing and Matls. (1973) 399.

50. W. Van Witzenburg, A. Mastenbroek, and J. D. Elen, J. Nucl. Mater., 104 (1981) 1187.

51. J. Bentley and F. W. Wiffen, Nucl. Tech., 30 (1976) 376.

52. M. P. Tanaka, E. E. Bloom, and J. A. Horak, J. Nucl. Mater. 103 & 104 (1981) 895.

53. F. W. Wiffen, ADIP Semiannual Progress Report, DOE/ER-0045/7 (1981) 145.

54. F. W. Wiffen, ADIP Quarterly Progress Report, DOE/ET-0058/1 (1978) 142.

55. F. W. Wiffen, in Defects and Defect Clusters in BCC Metals and Thir Alloys, Nucl. Metallurgy, 18 (1973) 179.

56. J. A. Horak, "Mechanical Properties of Irradiated V-20 wt.% Ti," ORNL-5082 (1975) and J. A. Horak and F. W. Wiffen, Mechanical Properties and Swelling of V-20% Ti," ORNL-5154, CTR Annual Report (1975).

57. Y. Adda, Radiation Induced Voids in Metals, J. W. Corbett and L. C. Ianniello, Eds., CONF-710601 (1972) 31.

58. R. B. Adamson, W. L. Bells, and P. C. Kelly, J. Nucl. Mater., 92 (1980) 149.

59. J. L. Brimhall and H. E. Kissinger, Radiation Effects, 15 (1972) 259.

60. M. Labbe, and J. P. Poirier, J. Nucl. Mater., 46 (1973) 86.

61. M. J. Makin, Voids Formed by Irradiation of Reactor Materials, S. F. Pugh, Ed., British Nuclear Energy Society (1971) 269.

62. R. Koch, R. P. Wahi, and H. Wollenberger, J. Nucl. Mater., 104 (1981) 1211.

63. M. J. Makin, Radiation Effects, W. F. Sheely, Ed., Metallurgical Society Confs., Vol. 37 (1965) 627.

64. J. N. Brooks, Nucl. Tech.-Fusion, 4 (1983) 33.